American Transactions on
Engineering & Applied Sciences

http://TuEngr.com/ATEAS

SaFaRiLAB: A Rugged and Reliable Optical Imaging System Characterization Set-up for Industrial Environment

Luisa De Marco [a], Anna Guagliumi [a], Marco Gnan [a,c], Bassam Hallal [b,d], Federico Canini [b], and Paolo Bassi [a*]

[a] *Dipartimento di Elettronica, Informatica e Sistemistica, Alma Mater Studiorum - University of Bologna, Viale del Risorgimento 2, I 40136 Bologna, Italy*

[b] *Datalogic Scanning Group s.r.l.,Via San Vitalino 13, I 40012 Lippo di Calderara di Reno BO, Italy*

[c] Present address: *Datalogic Scanning Group s.r.l.,Via San Vitalino 13, I 40012 Lippo di Calderara di Reno BO, Italy*

[d] Present address: *Khatod s.r.l., Via Monfalcone 41, I 20092 Cinisello Balsamo MI, Italy*

ARTICLEINFO

Article history:
Received 15 December 2011
Accepted 20 January 2012
Available online
21 January 2012

Keywords:
Incoherent imaging systems,
Characterization,
Spatial Frequency Response,
Modulation Transfer Function,
ISO 12233.

ABSTRACT

This work proposes a rugged and reliable set-up to characterize incoherently illuminated optical imaging systems. It complies with the ISO 12233 standard and is suitable for industrial applications. The standard has been implemented taking advantage of the allowed degrees of freedom to optimize noise robustness. Key points of the algorithm are automatization of the whole measurement procedure and customization, to comply with specific needs. Experimental results confirming the successful implementation are presented and discussed.

*Corresponding author (**Paolo Bassi**). Tel +39-051-2093050 Fax: +39-051-2093053 E-mail address: paolo.bassi@unibo.it. © 2012. American Transactions on Engineering & Applied Sciences. Volume 1 No.1 ISSN 2229-1652 eISSN 2229-1660. Online Available at http://TUENGR.COM/ATEAS/V01/91-105.pdf

1. Introduction

Theoretical and experimental characterization of optical imaging systems is important in many classical applications, such as, for example, photography or microscopy, but also in emerging ones, such as those belonging to the biological and medical fields. Theoretical analysis of imaging systems can be done using linear system theory concepts both for coherent and incoherent illumination [Goodman]. Much scientific and technical literature has been devoted to the problem of their characterization (see, for example [Coltman, Park, Boreman 1995, Estribeau, Ducharme]). On the whole, the possibility to use linear system analysis, greatly simplifies the task, since one can develop approaches in the spatial coordinate system, using the system impulse response, referred to as Point Spread Function (PSF), or in the spatial frequency domain, using the Spatial Frequency Response (SFR).

Application of these approaches in the industrial environment introduces a further challenge, related to the need of rugged and versatile tools that may withstand hostile environments and to the need for adapting the measurement set-up to different applications. This generally leads to the definition of International Standards referring to specific problems. In this paper we will refer to the ISO 12233 standard on Photography, Electronic Still Picture Cameras, Resolution Measurements [ISO 12233], which considers optical systems with incoherent illumination.

Many implementations of this standard are available. They can be freely distributed (for example as a plugin for IMAGEJ [ImageJ], based on the Java language, MITRE [Mitre] based on the C language, and SFRMAT [SFRmat], based on Matlab) or commercially distributed (for example IMATEST [Imatest] and QUICKMTF [QuickMTF]). Since the standard describes only guidelines for both the measurement conditions and the algorithm that calculates the SFR, it leaves degrees of freedom over its actual implementation that may impact on the overall results. In particular, the freely available packages are certainly easily customizable, but may be poorly documented and then should be anyway tested in depth before use, for example to determine their accuracy. On the contrary, commercially distributed ones allow no control on their algorithms and therefore it is impossible to customize them for specific needs, such as integrating them in portable devices.

In this paper, we present SAFARILAB (SFR measurement for a LAB environment), our

implementation of the ISO 12233 standard that, further than complying with the standard and guaranteeing versatility also in an embedded environment, addresses various critical points in its implementation and use, such as accuracy of the results and robustness to noise. In this way it allows the correspondence of the measured features to the designed ones and becomes rugged and reliable, therefore suitable for an industrial environment.

The paper is organized as follows: section 2 describes the developed software tool in detail. Then its performance is illustrated and compared with other available software using synthetic (section 3) and experimental (section 4) images. After assessing the features of the software with respect to noise (section 5), results of a case study are demonstrated in section 6. Finally, conclusions are drawn in section 7.

2. Algorithm for SFR evaluation

The ISO 12233 Standard concerns the measurement of the SFR of an incoherent imaging system. In the case of incoherent illumination, the principles describing linear systems can be applied simply using field intensities instead of field amplitudes [Goodman]. Measurement results, however, include not only the response of the optical part of the system to be characterized but also those of the other elements of the imaging chain, such as the detector (characterized by the finite pixel size of the used CCD camera) and the electronics [Boreman 2001]. The overall system SFR may be expressed as:

$$\mathrm{SFR}(f_x, f_y) = G_o(f_x, f_y) \cdot G_d(f_x, f_y) \cdot G_e(f_x, f_y) \quad (1)$$

where G_o is the contribution of the optical part of the system, G_d is related to the detector and G_e represents the electronic post-processing. If only one of these contributions is needed, for example the optical one, the others have to be evaluated and eliminated. This issue will be addressed later comparing measurements and simulations.

Rather than using a point source for direct PSF measurement, the ISO 12233 standard suggests

*Corresponding author (**Paolo Bassi**). Tel +39-051-2093050 Fax: +39-051-2093053 E-mail address: paolo.bassi@unibo.it. Volume 1 No.1 ISSN 2229-1652 eISSN 2229-1660. Online Available at http://TUENGR.COM/ATEAS/V01/91-105.pdf

to evaluate the SFR of an imaging system using a knife-edge source, thus reducing the analysis to a 1D problem. This method has proven to combine flexibility and simplicity, which are important features in any standard definition.

The corresponding system response is named Edge Spread Function (ESF) and is related to the SFR by derivative and Fourier transform operations:

$$\mathrm{SFR}(f_x) = \mathcal{F}\{LSF(x)\} = \mathcal{F}\left\{\frac{d}{dx} ESF(x)\right\} \quad (2)$$

where LSF stands for Line Spread Function and is the response of the system to a line source.

The standard recommends the use of an edge slanted at 5° with respect to the relevant coordinate axis in order to allow for the super-resolution of the ESF during the post-processing of the detected image, as it will be explained below, thus reducing the aliasing effects created by the sensor sampling.

The following algorithm steps, implemented by SAFARILAB, include those recommended by the standard ISO 12233 and complete them by focusing on noise and sampling issues important for the accuracy of the SFR evaluation:

1. *Image acquisition and averaging.* A number of images is acquired and averaged as to reduce the amount of noise. The average image is then cropped as to select the Region Of Interest (ROI) that contains the slanted edge to be processed in the following steps.
2. *Estimation of the edge slope*. The slope of the slanted edge is recovered with high precision via a linear regression operation on the so-called centroids, the peaks of the derivatives of each image line (LSF). To reduce noise effects, the LSF of each line is tapered using an asymmetrical Hamming window before centroids determination. This operation is repeated until the angle estimation achieves a precision of 10^{-6} degrees.
3. *Edge super-resolution.* By considering the image lines as independent sampled repetitions of the same ESF, an oversampled ESF is created. As it is shown in Figure 1, the information on the edge slope allows to find the relative offset among each ESF line, which in turn allows to

use them to create a super-resolved ESF with irregular sampling. Then, groups of data points are averaged to obtain the oversampled ESF having regular sampling with the desired super-resolution factor. This parameter, that the standard suggests to be 4, can be adjusted in our implementation.

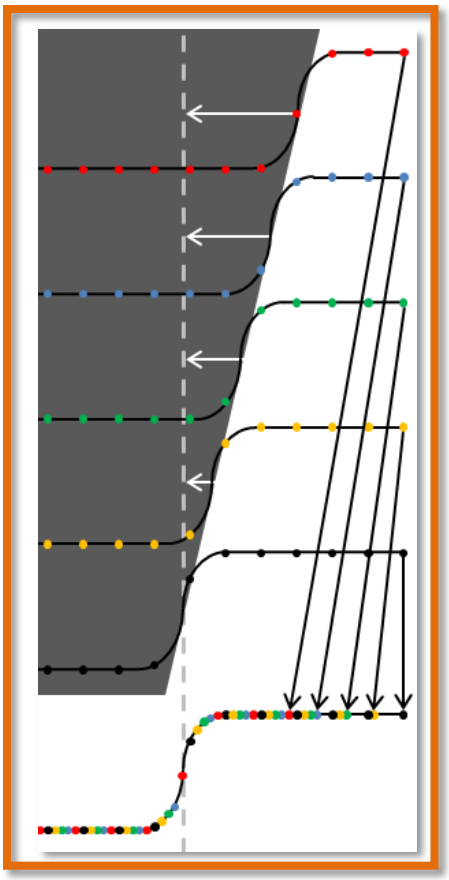

Figure 1: Creation of the oversampled ESF.

4. *LSF calculation* as the numerical derivative of the oversampled ESF, multiplied by an asymmetrical Hamming window.
5. *SFR calculation* as the Fourier transform of the LSF.
6. *SFR averaging*. A number of SFRs are obtained by repeating the previous steps and are averaged to improve the accuracy of the estimation.

Within these steps many parameters (such as the number of images on which to average the input to the tool, the super-resolution factor and the number of SFR calculations) are related to the

*Corresponding author (**Paolo Bassi**). Tel +39-051-2093050 Fax: +39-051-2093053 E-mail address: paolo.bassi@unibo.it. Volume 1 No.1 ISSN 2229-1652 eISSN 2229-1660. Online Available at http://TUENGR.COM/ATEAS/V01/91-105.pdf

accuracy of the extraction of the SFR. It is important that their values are correctly set.

In the remainder of the paper, the behavior of SAFARILAB is demonstrated. Initially accuracy tests are shown in which the software is used on numerically created images (synthetic) and on images obtained by real optical systems. In both cases, its results are compared to those of two available tools: IMAGEJ and IMATEST. Finally, an example of use in a real test case is given.

3. SFR extraction from synthetic images

The initial verification of the performance of SAFARILAB is done using as its input a numerically created image, in which the black-to-white transition follows an analytically known function to allow comparison of obtained results with exact, reference, ones. The arctangent function has been used since it satisfies the following requirements:

- It has the same qualitative shape of a real edge.
- The analytical expression of the convolution with a rectangular window (to include the sampling effect) is known:

$$\begin{aligned}\arctan(x) \star \mathrm{rect}\left(\frac{x}{T}\right) &= \int_{-\infty}^{+\infty} \arctan(x-\tau)\, rect\left(\frac{\tau}{T}\right) d\tau = \int_{-T/2}^{T/2} \arctan(\mathrm{x}-\tau)\mathrm{d}\tau = \\ &= -\left(x-\frac{T}{2}\right)\arctan\left(x-\frac{T}{2}\right)+\left(x+\frac{T}{2}\right)\arctan\left(x+\frac{T}{2}\right)+ \\ &+\frac{1}{2}\ln\left[\left(x-\frac{T}{2}\right)^2+1\right]-\frac{1}{2}\ln\left[\left(x+\frac{T}{2}\right)^2+1\right]. \end{aligned} \quad (3)$$

- The derivative of this convolution is also analytically known:

$$\frac{d}{dx}\left[\arctan(x) \star \mathrm{rect}\left(\frac{x}{T}\right)\right] = \frac{1}{\mathrm{x}^2+1} \star \mathrm{rect}\left(\frac{x}{T}\right). \quad (4)$$

- The analytical expression of the Fourier transform of this derivative, which is the SFR, exists:

$$\mathcal{F}\left\{\frac{1}{\mathrm{x}^2+1} \star \mathrm{rect}\left(\frac{x}{T}\right)\right\} = \pi e^{-|2\pi f_x|} \cdot \mathrm{sinc}(f_x T). \quad (5)$$

To make the image more realistic, we also added shot noise, as it is typically the most relevant

noise contribution given by photo-sensors. Noise is modeled as a Poisson process with mean value and standard deviation dependent on the signal.

Supposing to use 8 bit A/D conversion, a black and white image has pixels with values ranging from 0 to 255. In order to simulate measurements with large contrast and zero-mean noise, synthetic slanted-edge images have been created assuming a linear Opto-Electronic Conversion Function (OECF) leading to an image with grey levels in the range 30-220.

Evaluated SFRs are shown in Figure 2 using logarithmic plots. Spatial frequencies are normalized (as in the rest of the paper) to half of the reciprocal of the sampling step (i.e. the Nyquist frequency). The red curve is the theoretical SFR, while the other three are obtained using different software: IMATEST (black line), IMAGEJ (blue line) and SAFARILAB (green line).

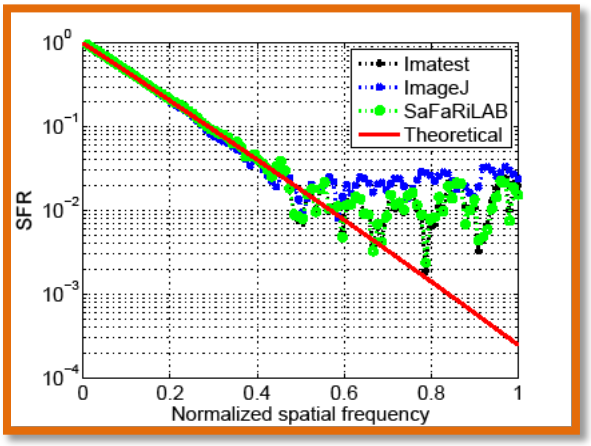

Figure 2: Test with synthetic images with additional noise and contrast of 30-220 (red: theoretical; black: IMATEST; blue: IMAGEJ; green: SAFARILAB).

The three tools show similar degree of accuracy, with IMAGEJ performing slightly differently from the other two. In all cases, the presence of noise produces small oscillations in the SFRs as compared to the theoretical curve when the normalized frequency is greater than 0.5 and the SFR is lower than 0.02. The slight mismatch between the results obtained using IMATEST and IMAGEJ is directly related to the degrees of freedom allowed by the standard. The good agreement between these results and those obtained by SAFARILAB confirms the correctness of our algorithms. The next sections will show how the freedom left by the standard can be exploited to improve the

*Corresponding author (**Paolo Bassi**). Tel +39-051-2093050 Fax: +39-051-2093053 E-mail address: paolo.bassi@unibo.it. Volume 1 No.1 ISSN 2229-1652 eISSN 2229-1660. Online Available at http://TUENGR.COM/ATEAS/V01/91-105.pdf

quality of the provided results. Evidence will be given by experimental results.

4. SFR extraction on real images

Real images are acquired using the set-up shown in Figure 3 (left). A slanted-edge transmission mask, made of chrome deposited on glass (right side of Figure 3), is uniformly illuminated by an incoherent source obtained by cascading two integrating spheres and a LED source. The image of the edge is acquired by the imaging system to be characterized, consisting of a lens, a photo-detector and its relevant driver electronics.

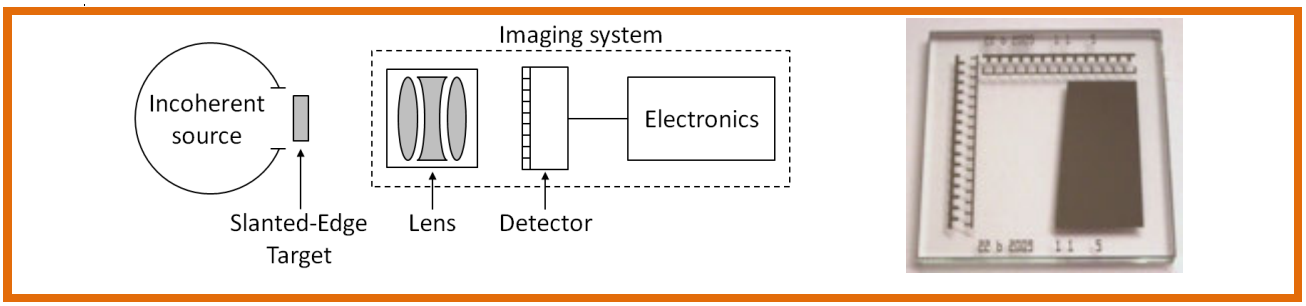

Figure 3: Measurement set-up scheme (left) and Slanted Edge target (right).

Figure 4 shows the SFR extracted from slanted-edge images taken with a distance of 190 mm between the mask and camera. The packages applied to experimental results always behave similarly: SAFARILAB (green plot) and IMATEST (black plot) results almost superimpose, while IMAGEJ (blue plot) is slightly different.

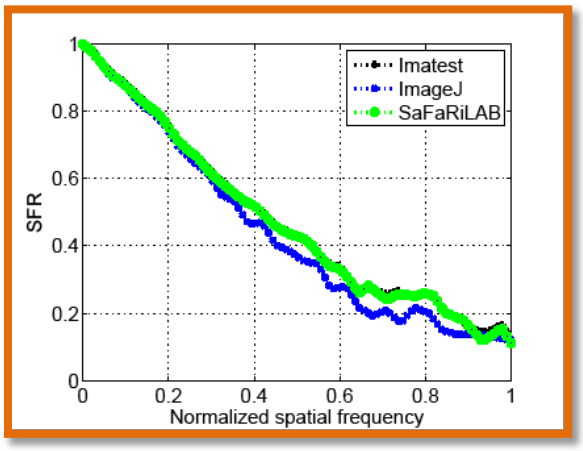

Figure 4: SFR obtained with experimental images taken at 190 mm from the target (black: IMATEST; blue: IMAGEJ; green: SAFARILAB).

Instead of using directly the SFR, often the performance of an optical system is given by its resolution on the object plane. The minimum feature size *R* that the system can resolve is inversely proportional to the spatial frequency at which the SFR reaches a threshold value, depending on system requirements. The formula to evaluate the minimum resolution is the following one:

$$R = \frac{1}{2 f_{th} M} \tag{6}$$

where f_{th} is the threshold frequency and *M* is the optical system magnification. In the following, f_{th} will be normalized with respect to the Nyquist frequency.

Since the measured SFR includes the response of the optics together with that of the electronic part of the system (equation (1)), the simulated SFRs were modified as include these contributions. The effect of the sensor sampling was considered the predominant one and was modeled as a *rect* function in the spatial domain or, equivalently, a *sinc* function in the spatial frequency domain.

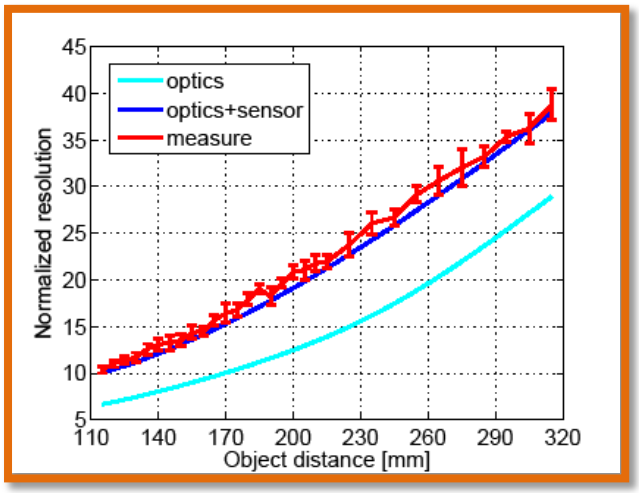

Figure 5: Comparison between designed (blue and cyan) and measured (red) performance. Resolution is normalized to the Nyquist frequency of the sensor.

Figure 5 shows an example of application of the procedure. The measured resolution of the camera as a function of the camera-target distance (red curve) is compared to that of the lens (cyan curve) and to that of the system composed by the lens and the sensor (blue curve). As it will be better explained in the next section, in order to remove noise effects the measured resolution is

*Corresponding author (**Paolo Bassi**). Tel +39-051-2093050 Fax: +39-051-2093053 E-mail address: paolo.bassi@unibo.it. Volume 1 No.1 ISSN 2229-1652 eISSN 2229-1660. Online Available at http://TUENGR.COM/ATEAS/V01/91-105.pdf

calculated by averaging 20 SFRs. The relevant uncertainty bars are also reported. The curve that represents the lens and the sensor system is just within the error bars of the measured resolution curve, confirming the quality of the results. With reference to Equation (1), Figure 5 also shows that the electronics has a negligible effect on the overall system performance.

5. Noise reduction

The noise in the image entering the processing chain introduces uncertainty to the SFR extraction. In order to improve the accuracy, an average SFR is found by repeating the extraction process. Figure 6 (left) shows a set of 20 SFR curves (green lines) calculated from 20 different slanted-edge images together with their average (solid red line) and average ±3σ(f) (dashed red lines), where σ(f) is the standard deviation as a function of the spatial frequency f. The image noise causes noise-like oscillations into the SFR so that averaging appears as a necessary step for a reliable evaluation of the SFR.

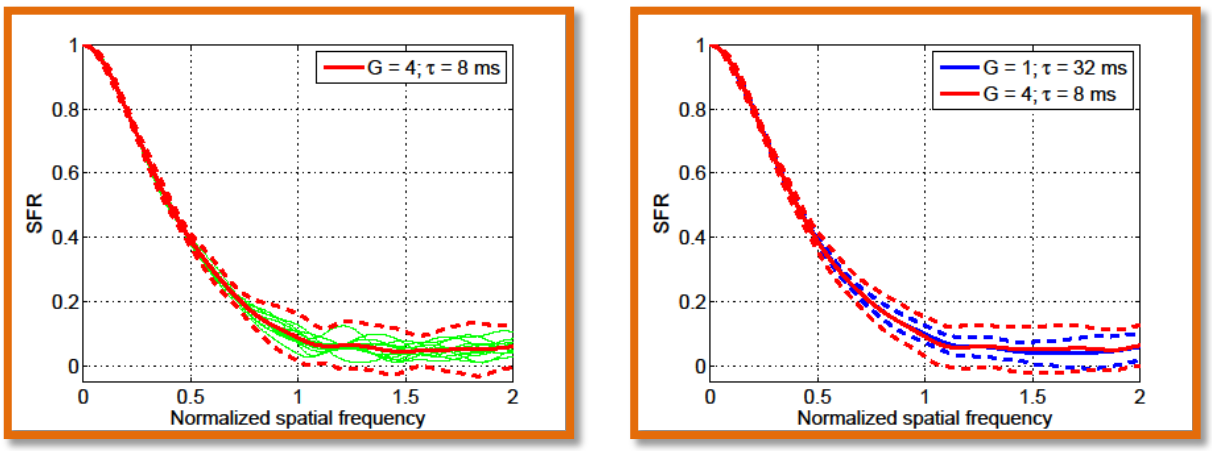

Figure 6: Noise effects on SAFARILAB responses (see text for details).

The influence of different noise levels has also been considered by changing the analog gain (G) and the integration time (τ) of the camera: lower gain and higher integration time correspond to a noise reduction. In the right part of Figure 6, the red curves are obtained with analog gain G = 4 and integration time τ = 8 ms (the same conditions of Figure 5-right), whereas the blue curves are obtained with G = 1 and τ = 32 ms. The solid curves represent the average SFR (calculated as the average of 50 SFR), whereas the dashed curves represent the average SFR ±3σ(f). As expected, the uncertainty is greater in the first case since noise is larger. Averaging 50 SFRs, SAFARILAB is able

to recover the same mean value in both cases, thus demonstrating a good insensitivity to random noise effects.

However, it is sometimes impossible to control the analog gain and the integration time in the needed way. To overcome this limit and obtain the same effect of noise reduction without acting on the camera parameters, SAFARILAB may also make image averaging as the very first step of its algorithm. The number of images to be averaged should be chosen in relation with the number of SFR evaluations for the calculation of the average, since both impacts on the overall execution time.

6. Characterization of a system using SAFARILAB

After the description of SAFARILAB capabilities evidencing the original way in which noise contributions can be filtered differently depending on the experimental situation, in this section its versatility will be demonstrated on an optical system containing also non-classical components designed to achieve Extended Depth of Field (EDoF). Among the possible ways of getting this result, see for example [McLeod, Kolodziejczyk, Davidson, Andersen, Iemmi], we adopted the so called "Wavefront Coding" approach [Dowski], based on the insertion of a Phase Mask (PM) into the optical system. Among the proposed solutions, see for example [Dowski, Sauceda, Sherif, Caron, Zhou], we have chosen the cubic one [Dowski] since it has also a solid theoretical background which may be useful in simulations. The cubic profile is described by:

$$z = \alpha(x^3 + y^3) \tag{6}$$

where x and y are the planar spatial coordinates and α is a cubic coefficient.

In the following, the SFR of a lens with and without a cubic phase mask is characterized using SAFARILAB. The match between designed and measured performance will confirm the reliability of the characterization tool itself.

The experimental curves are obtained by SAFARILAB as the average of 10 SFRs, each calculated on the average of 10 images. Also in this case the sensor sampling effect is included in the designed SFRs before comparing them with the measured ones.

*Corresponding author (**Paolo Bassi**). Tel +39-051-2093050 Fax: +39-051-2093053 E-mail address: paolo.bassi@unibo.it. Volume 1 No.1 ISSN 2229-1652 eISSN 2229-1660. Online Available at http://TUENGR.COM/ATEAS/V01/91-105.pdf

Figure 7 qualitatively shows the behavior of the system with (red curves) and without (blue curves) the phase mask. The plot on the left represents the designed SFR of the system for different object distances: the cubic mask provides a good invariance of the SFR, which corresponds to an extension of the DoF. The same behavior is shown also in the plot on the right obtained characterizing the real system with SAFARILAB.

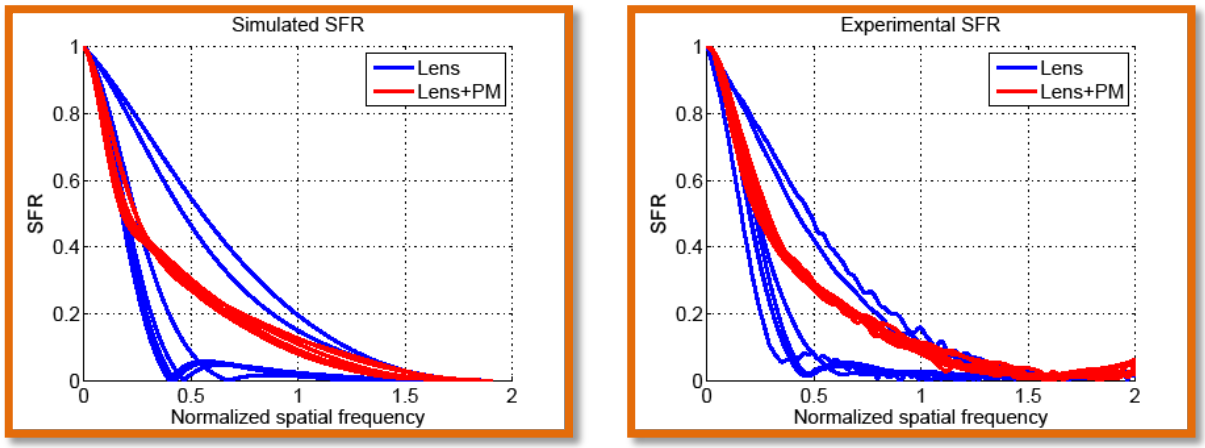

Figure 7: Simulated (left) and experimental (right) SFRs for the lens with (red lines) and without (blue lines) the cubic phase mask.

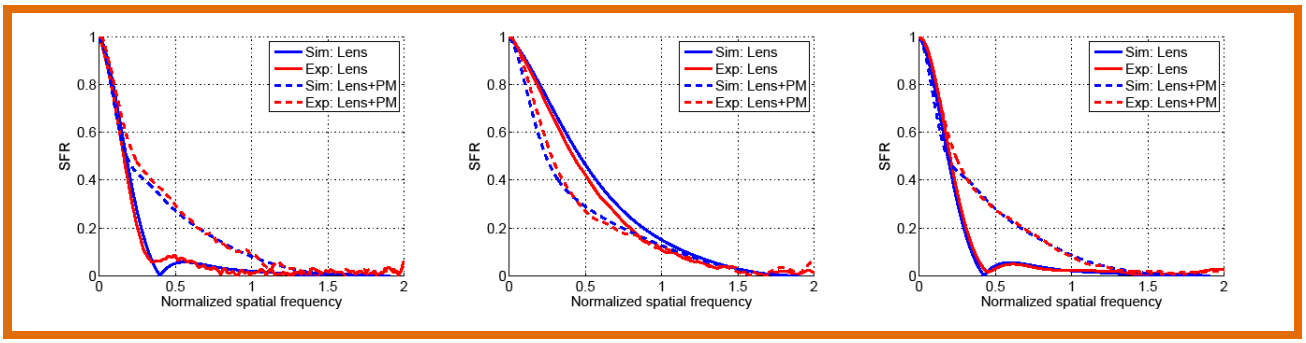

Figure 8: Simulated (blue) and measured (red) results with (dashed) and without (solid) phase mask. The object distance increases moving from the leftmost to the rightmost plot.

A more detailed view of the agreement between the expected behavior and the obtained one is given in Figure 8. The designed SFRs of the system with and without the phase mask at increasing object distances are compared to the ones measured with SaFaRiLAB. The excellent agreement between simulated and experimental curves confirms how our tool is accurate and useful in the design and analysis stage of an optical system.

7. Conclusion

A tool named SAFARILAB has been proposed. It evaluates the Spatial Frequency Response of an optical system complying with the ISO 12233 standard, the reference standard for this kind of measurements. Its performance has been first successfully compared with those of other available software dedicated to this task. Then, an experimental set-up has been realized to perform the measurements and the results show excellent behavior in terms of repeatability. The robustness to noise, obtained taking advantage of the degrees of freedom left by the standard, has also been evidenced. Finally, its reliability in a practical case has been proven comparing the measured optical SFRs and the designed ones in a more complex case where also a cubic phase mask is present. SAFARILAB can then be proposed as a valid tool for industrial environments and embedded systems, where noise robustness and versatility are both a concern.

8. Acknowledgements

This work has been developed in the framework of a research contract between DEIS and Datalogic Scanning Group.

9. References

Andersen, G. (2005). Large optical photon sieve. *Optics Letters*, 30(22), 2976-2978.

Boreman, G. D. and S. Yang. (1995). Modulation Transfer-Function measurement using 3-bar and 4-bar targets. *Applied Optics*, 34(34), 8050-8052.

Boreman, G. D. (2001). Modulation Transfer Function in Optical and Electro-Optical Systems. *SPIE Pres*s.

Caron, N. and Y. Sheng. (2008). Polynomial phase masks for extending the depth of field of a microscope. *Applied Optics*, 47(22), 39-43.

Coltman, J. W. (1954). The Specification of Imaging Properties by Response to a Sine Wave Input. *Journal of the Optical Society of America*, 44(6), 468-471.

Davidson, N., A. Friesem and E. Hasman. (1991). Holographic axilens: high resolution and long focal depth. *Optics Letters*, 16(5), 523-525.

Dowski, E. R. and W. T. Cathey. (1995). Extended depth of field through wave-front coding.

*Corresponding author (**Paolo Bassi**). Tel +39-051-2093050 Fax: +39-051-2093053 E-mail address: paolo.bassi@unibo.it. Volume 1 No.1 ISSN 2229-1652 eISSN 2229-1660. Online Available at http://TUENGR.COM/ATEAS/V01/91-105.pdf

Applied Optics, 34(11), 1859-1866.

Ducharme, A. D. and S. P. Temple. (2008). Improved aperture for modulation transfer function measurement of detector arrays beyond the Nyquist frequency. *Optical Engineering*, 49(7), 093601.

Estribeau, M. and P. Magnan. (2004). Fast MTF measurement of CMOS imagers using ISO 12233 slanted-edge methodology. *Proceedings of SPIE - Volume 5251 - Detectors and Associated Signal Processing*, 243-252.

Goodman, J. W. (2004). Introduction to Fourier Optics. 3rd Ed., *Roberts & Company Publishers*.

Iemmi, C., J. Campos, J. Escalera, O. López-Coronado, R. Gimeno and M. J. Yzuel. (2006). Depth of focus increase by multiplexing programmable diffractive lenses. *Optics Express*, 14(22), 10207-10219.

IMAGEJ (Image Processing and Analysis in Java) available at: http://rsbweb.nih.gov/ij/.

IMATEST software, available at: http://www.imatest.com/products/software/master.

ISO 12233 Standard (Photography - Electronic Still Picture Cameras - Resolution Measurements), available at: http://www.iso.org/iso/catalogue_detail.htm?csnumber=33715.

Kolodziejczyk, A., S. Bará, Z. Jaroszewicz and M. Sypek. (1990). The Light Sword Optical Element - a New Diffraction Structure with Extended Depth of Focus. *Journal of Modern Optics*, 37(8), 1283-1286.

McLeod, J. H. (1954). The Axicon: A New Type of Optical Element. *Journal of the Optical Society of America*, 44(8), 592-597.

MITRE, available at: http://www.mitre.org/tech/mtf/.

Park, S. K., R. Schowengerdt and M.A. Kaczynski. (1984). Modulation-transfer-function analysis for sampled image systems. *Applied Optics*, 23(15), 2572-2582.

QUICK MTF, available at http://www.quickmtf.com/.

SFRMAT (a Matlab function to provide the Spatial Frequency Response) available at: http://www.losburns.com/imaging/software/SFRedge/index.htm.

Sauceda, A. and J. Ojeda-Castañeda. (2004). High focal depth with fractional-power wave fronts. *Optics Letters*, 29(6), 560-562.

Sherif, S. S., W. T. Cathey and E. R. Dowski. (2004). Phase plate to extend the depth of field of incoherent hybrid imaging systems. *Applied Optics*, 43(13), 2709-2721.

Zhou, F., G. Li, H. Zhang and D. Wang. (2009). Rational phase mask to extend the depth of field in optical-digital hybrid imaging systems. *Optics Letters*, 34(3), 380-382.

Luisa De Marco received the B.Sc. and the M.Sc. degrees in Telecommunications Engineering from the University of Padova in 2006 and from the Alma Mater Studiorum – University of Bologna in 2008, respectively. She is currently working towards the PhD with a scholarship funded by Datalogic Scanning s.r.l. at the Dipartimento di Elettronica, Informatica e Sistemistica (DEIS) of the Alma Mater Studiorum – University of Bologna. In the framework of her doctoral research, she spent 6 months working at the Friedrich-Alexander University of Erlangen, Germany. Her main interest is the optical design of imaging and non-imaging systems for automatic identification and portable devices.

Anna Guagliumi received her M.Sc. degree (honors) in Telecommunication Engineering from the Alma Mater Studiorum – University of Bologna in 2010. Since 2011 she has been a PhD student at the Dipartimento di Elettronica, Informatica e Sistemistica (DEIS) of the Alma Mater Studiorum – University of Bologna. Her main interests are the design and characterization of optical structures, especially with respect to free space systems.

Marco Gnan received the M.Sc. degree (honors) in Telecommunication Engineering from the Alma Mater Studiorum – University of Bologna. From 2003 he worked towards the PhD in Optoelectronics at the University of Glasgow, which he achieved in 2007. Until February 2008 he was with the Department of Engineering at the University of Ferrara as a research assistant. Until December 2011 he was with the Dipartimento di Elettronica, Informatica e Sistemistica of the University of Bologna as a senior research assistant. Since January 2012 he has been with the R&D group of Datalogic. His interests include experimental work on integrated photonic devices and their numerical modeling, free space optics and incoherent imaging systems.

Bassam Hallal received the M.Sc. degree in Electronic Engineering (honors) from the Politecnico di Bari in 1997 extending the Knoesen-Gaylord-Moharam algorithm for the analysis of the hybrid guided modes to the uniaxial dielectric multilayered waveguides. In 1998 he received a Master in Optical Technologies from the AILUN (Associazione Istituzione Libera Università Nuorese). He spent the years 1999-2011 in Datalogic working on diffraction-free beams synthesis, pure refractive aiming systems, lens design for imaging systems, CCD/CMOS sensors characterization, and free-form lens design. Since December 2011 he has been with Khatod s.r.l. as the Optical R&D Supervisor.

Federico Canini received the M.Sc. degree with honors in Electronic Engineering from the Alma Mater Studiorum – University of Bologna in 1994. In 1995 he started his activity in Datalogic covering many engineering roles, developing new products based on imaging technologies and producing several patents. He currently is an R&D manager at Datalogic IP Tech and is responsible for the electronic and the optics group, and the relationship with academic partners.

Paolo Bassi is full professor of Electromagnetic fields at Dipartimento di Elettronica, Informatica e Sistemistica (DEIS) of the Alma Mater Studiorum – University of Bologna. He graduated with honors in Electronic Engineering in 1975. He is now the responsible of the optics group of DEIS. His research interests cover guided and free space application of optics, addressed both theoretically and experimentally.

Peer Review: This article has been internationally peer-reviewed and accepted for publication according to the guidelines given at the journal's website.

*Corresponding author (**Paolo Bassi**). Tel +39-051-2093050 Fax: +39-051-2093053 E-mail address: paolo.bassi@unibo.it. Volume 1 No.1 ISSN 2229-1652 eISSN 2229-1660. Online Available at http://TUENGR.COM/ATEAS/V01/91-105.pdf